

## Relations between structural distortions and transport properties in $\text{Nd}_{0.5}\text{Ca}_{0.5}\text{MnO}_3$ strained thin films

This article has been downloaded from IOPscience. Please scroll down to see the full text article.

2002 J. Phys.: Condens. Matter 14 3951

(<http://iopscience.iop.org/0953-8984/14/15/309>)

View [the table of contents for this issue](#), or go to the [journal homepage](#) for more

Download details:

IP Address: 171.66.16.104

The article was downloaded on 18/05/2010 at 06:28

Please note that [terms and conditions apply](#).

# Relations between structural distortions and transport properties in $\text{Nd}_{0.5}\text{Ca}_{0.5}\text{MnO}_3$ strained thin films

E Rauwel Buzin, W Prellier, B Mercey, Ch Simon and B Raveau

Laboratoire CRISMAT, CNRS UMR 6508, 6 Bd du Maréchal Juin, 14050 Caen Cedex, France

E-mail: prellier@ismra.fr

Received 14 January 2002, in final form 13 March 2002

Published 4 April 2002

Online at [stacks.iop.org/JPhysCM/14/3951](http://stacks.iop.org/JPhysCM/14/3951)

## Abstract

Strained thin films of charge/orbital-ordered (CO/OO)  $\text{Nd}_{0.5}\text{Ca}_{0.5}\text{MnO}_3$  with various thicknesses have been grown on (100)  $\text{SrTiO}_3$  and (100)  $\text{LaAlO}_3$  substrates, by using the pulsed laser deposition technique. The thickness of the films drastically influences the transport properties. As the thickness decreases, the CO transition becomes more favoured while at the same time the insulator-to-metal transition temperature becomes less favoured under application of a 7 T magnetic field. Clear relationships between the structural distortions and the transport properties are established. They are explained on the basis of the elongation and the compression of the Mn–O–Mn and Mn–O bond angles and distances of the  $Pnma$  structure, which modify the bandwidth and the Jahn–Teller distortion in these materials.

## 1. Introduction

Perovskite-type manganites such as  $\text{R}_{1-x}\text{A}_x\text{MnO}_3$  (R = rare-earth ion and A = alkaline-earth ion) have been extensively investigated because of their colossal-magnetoresistance properties (CMR) [1]. The CMR effect originates from a competition between a ferromagnetic metallic (FMM) state and an antiferromagnetism insulating (AFMI) state. The appearance of the FMM state is explained by the double-exchange (DE) mechanism [2], whereas the AFMI state originates from Jahn–Teller (JT) distortions [3–5], leading in the case of small A-site cations to the charge/orbital-ordered (CO/OO) phenomenon [6]. The efforts made to understand the magnetotransport properties of manganite thin films [1, 7, 8] have shown that the physical properties are often different from those of the bulk materials. The main reason for this is the strains, including the substrate-induced strains, which modify the lattice parameters of the film and change the properties, as shown recently for  $\text{Pr}_{0.5}\text{Ca}_{0.5}\text{MnO}_3$  [9–11],  $\text{La}_{1-x}\text{Ba}_x\text{MnO}_3$  [12] and  $\text{Nd}_{0.5}\text{Ca}_{0.5}\text{MnO}_3$  [13].

In manganite thin films, the strains tend to modify the Mn–O–Mn angles and Mn–O distances. Consequently, this affects the bandwidth and also the JT distortions, so DE and

CO/OO phenomena may be strongly influenced. As a result of these factors, the strain effects should decrease as the thickness increases and it should be possible to establish relationships between the structural distortions and the transport properties, by studying the properties of films with various thicknesses.

Starting with  $\text{Nd}_{0.5}\text{Ca}_{0.5}\text{MnO}_3$  films, for which a spectacular CMR effect was previously evidenced [13], as compared to the bulk [14], we have carried out a systematic study of films with different thicknesses grown *in situ* using the pulsed laser deposition (PLD) technique on both (100)  $\text{SrTiO}_3$  and (100)  $\text{LaAlO}_3$  substrates. In this paper, a clear correlation is found between the structural distortions and the transport properties (an insulator-to-metal ( $T_{\text{IM}}$ ) transition under a magnetic field and a CO/OO ( $T_{\text{CO}}$ ) transition). We suggest that for small film thicknesses the elongation of the Mn–O bonds prevails, reinforcing the JT distortion and consequently the CO/OO state, whereas for large thicknesses a flattening of the Mn–O–Mn bond angles prevails, increasing the bandwidth and favouring the insulator-to-metal transition to the detriment of the CO/OO state.

## 2. Experimental procedure

Films with different thicknesses were deposited on single-crystal substrates of (100)  $\text{SrTiO}_3$  (STO) and (100)  $\text{LaAlO}_3$  (LAO) from dense targets of  $\text{Nd}_{0.5}\text{Ca}_{0.5}\text{MnO}_3$  using the PLD technique. Details of the process can be found elsewhere [13]. The structural study was done by means of x-ray diffraction (XRD) using a Seifert XRD 3000P for the  $\Theta$ – $2\Theta$  scans and a Phillips MRD X'pert for the in-plane measurements ( $\text{Cu K}\alpha$ ,  $\lambda = 1.5406 \text{ \AA}$ ). The in-plane lattice parameters were obtained from the  $(103)_{\text{C}}$  reflection (where C refers to the ideal cubic perovskite cell;  $a_{\text{C}} = 3.9 \text{ \AA}$ ). An electron microscope, JEOL 2010, equipped with an energy-dispersive spectroscopy (EDS) analyser, was used for the electron diffraction (ED) study. The EDS has shown that the cationic composition of the film is homogeneous and remains very close to the nominal one ' $\text{Nd}_{0.5\pm 0.02}\text{Ca}_{0.5\pm 0.02}\text{MnO}_x$ ' within experimental error.

The resistivity ( $\rho$ ) of the films was measured with a Quantum Design PPMS as a function of the magnetic field ( $H$ ) and the temperature ( $T$ ) using four-probe contacts. The thickness ( $t$ ) of the films is measured using a Dektak<sup>3</sup>ST surface profiler.

Besides the classical growth parameters, such as the deposition temperature and the oxygen pressure, we found that the energy of the laser was also important for obtaining a single phase. The optimum energy value is 200 mJ, which corresponds to  $2 \text{ J cm}^{-2}$  on the target. This is evidenced in figure 1 for a 2000  $\text{\AA}$  thick film of NCMO on STO. Low (132 mJ) or a high (240 mJ) laser energy leads to poor crystallization of the film with the appearance of a secondary phase.

## 3. Results

### 3.1. Structural properties

The structure of bulk NCMO is orthorhombic ( $Pnma$ ) with  $a = 5.4037 \text{ \AA}$ ,  $b = 7.5949 \text{ \AA}$  and  $c = 5.3814 \text{ \AA}$  [15]. Some areas of the film have been investigated by ED and we found that the films are single phase, [010] oriented, i.e. with the [010] axis perpendicular to the STO substrate plane, and [101] oriented, i.e. with the [101] axis perpendicular to the LAO substrate plane, in the space group  $Pnma$ . This orientation is not surprising, and results from the lattice mismatch between the film and the substrate as previously reported for  $\text{Pr}_{0.5}\text{Ca}_{0.5}\text{MnO}_3$  thin films grown on (100)  $\text{SrTiO}_3$  and (001)  $\text{LaAlO}_3$  substrates [9, 10]. Details of the transmission electron microscopy study currently being undertaken will be published elsewhere.

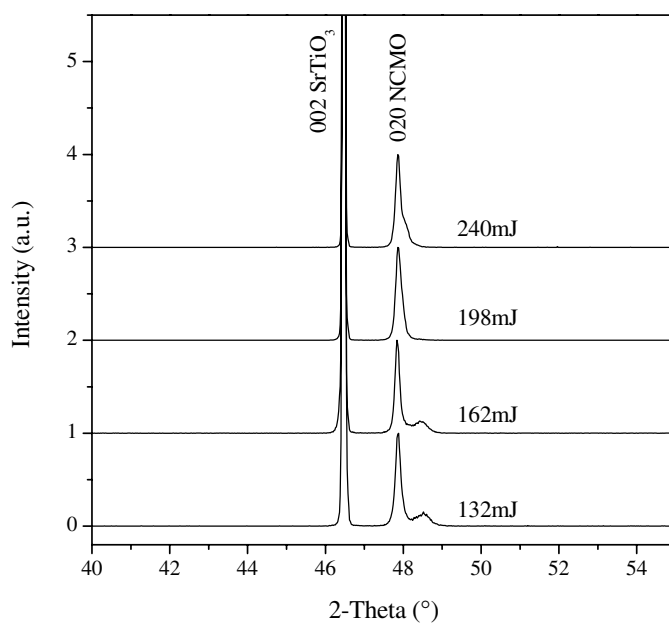


**Figure 1.** Room temperature XRD in the range  $40\text{--}55^\circ$  for a  $2000\text{ \AA}$  NCMO film on STO grown with various energies of the laser beam.

Figure 2(a) shows the evolution of the lattice parameters of the NCMO film grown on STO versus thickness. One observes that the in-plane lattice parameter  $d_{101}$  decreases as the thickness of the film increases while, at the same time, the out-of-plane lattice parameter  $d_{020}$  increases. The lattice parameters of films on LAO were also determined (figure 2(b)) but, due to the twins of these substrates, we were not able to obtain the in-plane lattice parameters. The out-of-plane lattice parameters remain almost constant on LAO while the thickness is changing, suggesting that the film is quasi-relaxed even for small thickness.

### 3.2. Transport properties

Figure 3(a) shows the resistivity dependence of the temperature for NCMO films on STO. Without a magnetic field, all films present semiconducting behaviour with an anomaly around  $275\text{ K}$ , corresponding to  $T_{\text{CO}}$ . A similar effect is observed for the bulk, but at a lower temperature close to  $250\text{ K}$  [17]. In fact, this anomaly in the  $\rho(T)$  curves is clearer (inset of figure 3(a)) when the resistance is plotted on a logarithmic scale versus the inverse of the temperature. On applying a magnetic field of  $7\text{ T}$ , while the thinner film ( $t = 670\text{ \AA}$ ) remains insulating over the whole temperature range of  $4\text{--}300\text{ K}$ , the thicker films ( $t > 1340\text{ \AA}$ ) show an insulator-to-metal transition ( $T_{\text{IM}}$ ) at  $100$  and  $130\text{ K}$  for the  $1340$  and  $2000\text{ \AA}$  films respectively. Such an effect is typical of the metastability of the CO/OO state where a magnetic field (called  $H_{\text{C}}$ ) can induce a metallic behaviour at low temperature. However, the magnetic field required is much higher for the bulk compound (close to  $20\text{ T}$  for the same temperature) [14]. In fact, there is a dependence of the critical field on the temperature (figure 3(b)). The resistivity shows a significant decrease on a logarithmic scale at a critical field ( $H_{\text{C}}$ ), indicating field-induced melting of the CO/OO state. This field-induced insulator-to-metal transition, which accompanies the collapsing of the CO/OO state, takes place below  $T_{\text{CO}}$ . This decrease can be viewed as indicating a CMR of about four orders of magnitude at  $75\text{ K}$ . A clear hysteresis (between the lower and the

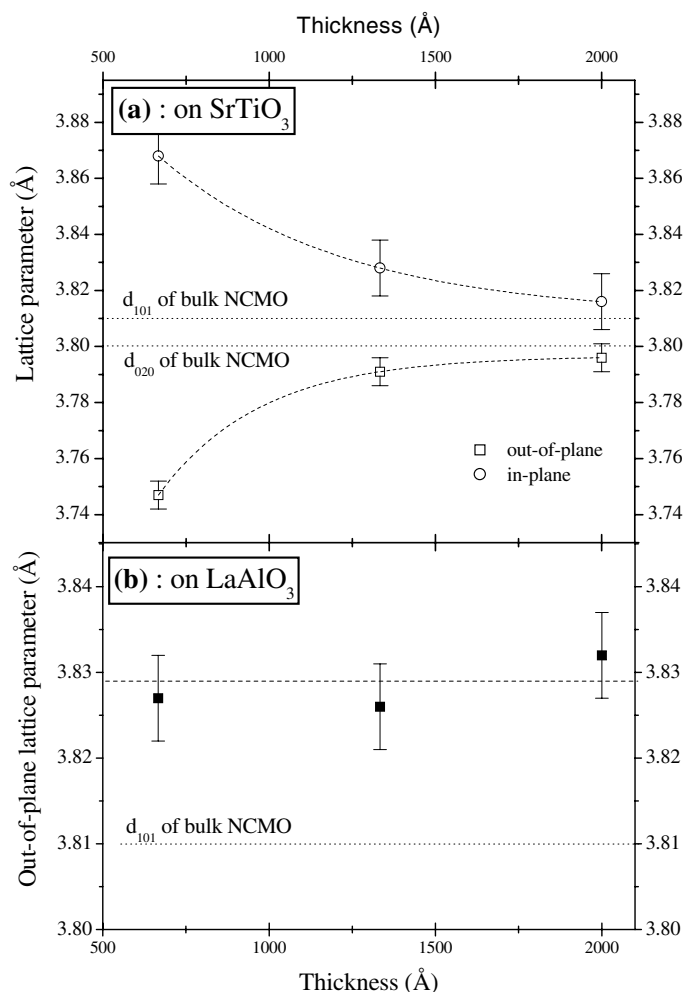


**Figure 2.** (a) Evolution of the lattice parameters of NCMO on STO as a function of the thickness. (b) Evolution of the out-of-plane lattice parameters of NCMO on LAO as a function of the thickness. The values for the bulk are indicated as dotted lines (see the text for details). Lines are only guides for the eyes.

upper critical fields) is seen at these temperatures, as previously reported for several CO/OO compounds [6, 18, 19], but this hysteretic region is more pronounced when the temperature is decreasing (see  $\rho(H)$  at 25 K in figure 3(b)). In addition, temperature dependence of a large-hysteresis region is a characteristic of a first-order transition and has been extensively studied for the composition  $\text{Nd}_{0.5}\text{Sr}_{0.5}\text{MnO}_3$  in [18]. Note also the re-entrant nature of the CO at 25 K, due to the fact that a 7 T magnetic field is not enough to completely melt this state.

On LAO substrates, the  $\rho(T)$  curves are almost the same (figure 4(a)) as those on STO, except that in this case, even the thinnest film (670 Å) displays an insulator-to-metal transition on applying a magnetic field of 7 T. Moreover,  $T_{\text{IM}}$  is higher than in the case of STO, which is consistent with the finding of a quasi-relaxed NCMO film on LAO (for a 1340 Å film,  $T_{\text{IM}} < 100$  K on STO and  $T_{\text{IM}} = 110$  K on LAO). Large hystereses indicating a first-order phase transition are also observed (figure 4(b)) and, in the same way, there is an increase of  $T_{\text{CO}}$  when the thickness of the film decreases (inset of figure 4(a)).

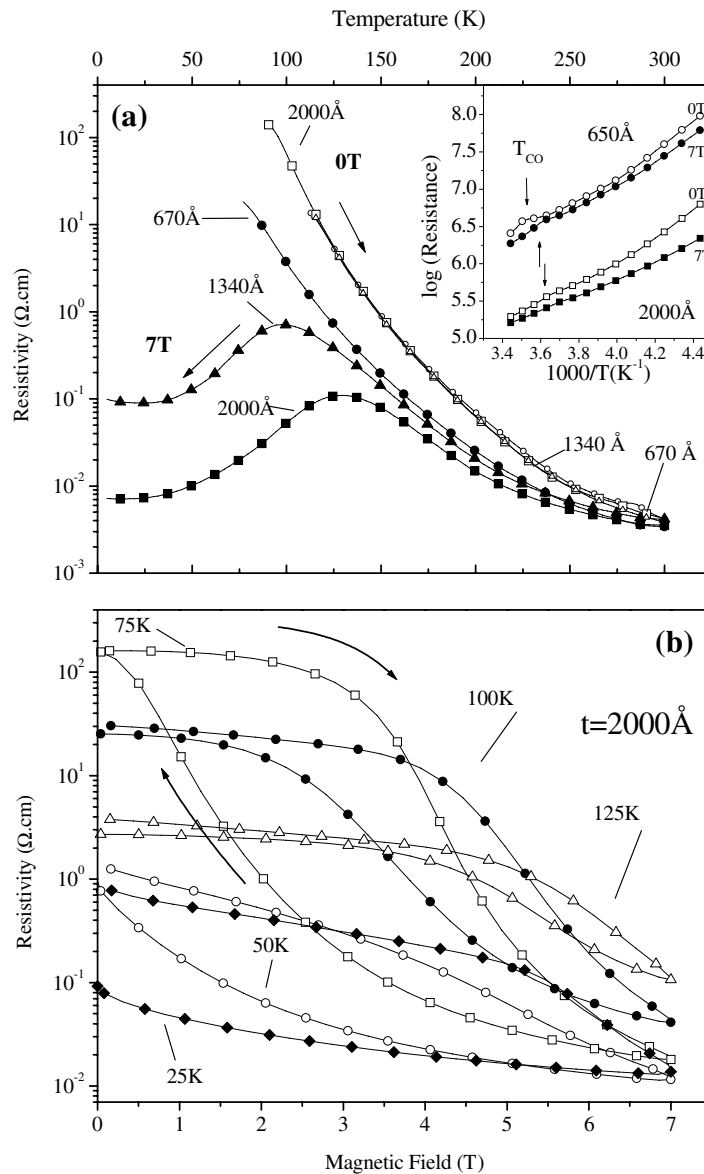


**Figure 3.** NCMO films on STO with various thicknesses. (a)  $\rho(T)$  under 0 T (open symbols) and 7 T (full symbols). The inset depicts the evolution of the logarithmic resistivity versus the inverse of the temperature under 0 T (open symbols) and 7 T (full symbols). Note the anomaly associated with  $T_{CO}$  (marked by an arrow). (b)  $\rho(H)$  at various temperatures for a 2000 Å film.

### 3.3. Discussion

This study shows that the thickness of the NCMO films deposited on STO strongly influences the transport properties of the material. For the largest thickness ( $t = 2000 \text{ \AA}$ ), an insulator-to-metal transition is induced under 7 T in contrast to the case for the bulk [14], although the cell parameters reach values close to those for bulk ceramics [15]. Moreover,  $T_{IM}$  under a 7 T magnetic field decreased as the thickness decreased whereas, at the same time,  $T_{CO}$  increases, so for a small thickness ( $t = 650 \text{ \AA}$ ) the film remains insulating.

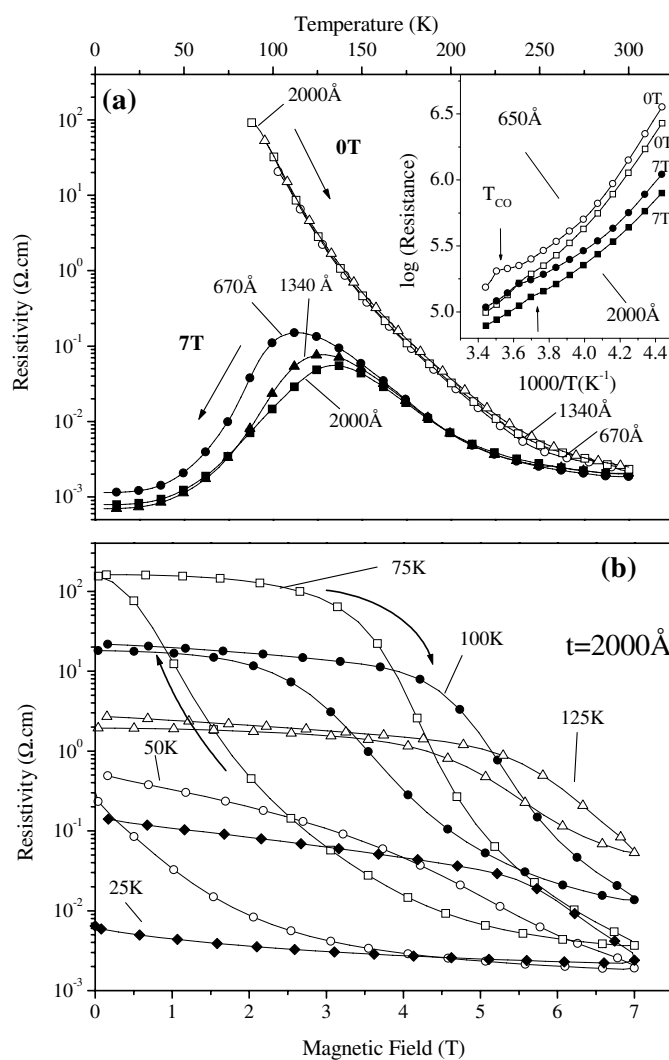


**Figure 4.** NCMO films on LAO with various thicknesses. (a)  $\rho(T)$  under 0 T (open symbols) and 7 T (full symbols). The inset depicts the evolution of the logarithmic resistivity versus the inverse of the temperature under 0 T (open symbols) and 7 T (full symbols). Note the anomaly associated with  $T_{\text{CO}}$  (marked by an arrow). (b)  $\rho(H)$  at various temperatures for a 2000 Å film.

Though it was suggested by several authors, for bulk samples of the same composition, that electronic phase separation could be the origin of the drop in resistivity [15, 16], no evidence of such phase separation was found in the thin films. We have indeed observed a continuous variation of the lattice parameters with the thickness of the films.

Thus, in order to explain this evolution, we have taken into consideration the following features concerning the strains induced by the STO substrates:

- (i) The tensile stain along the [101] direction (in the plane of the substrate) can increase both the Mn–O–Mn angles and the Mn–O distances in the equatorial plane (see figure 5(a)). Increase of the<sup>1</sup> Mn–O<sub>EQ</sub>–Mn bond angle increases the bandwidth [20], the angles tending

<sup>1</sup> O<sub>EQ</sub> and O<sub>AX</sub> refer respectively to the equatorial and axial oxygens (see figures 4(a)–(b)).

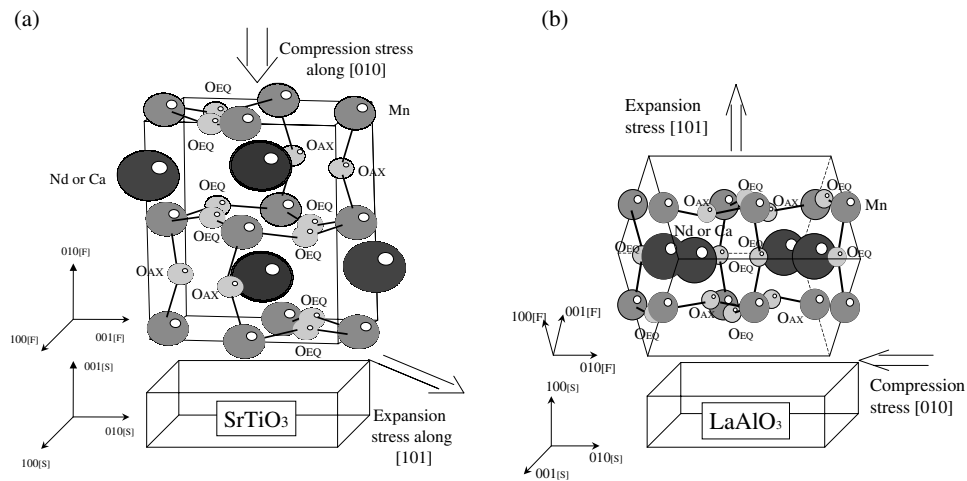


**Figure 5.** (a) Idealized [010] NCMO structure on STO. The directions of the stress are indicated by arrows. F and S refer to the film and to the substrate. (b) Idealized [101] NCMO structure on LAO. The directions of the stress are indicated by arrows. F and S refer to the film and to the substrate.

toward  $180^\circ$ , so DE is involved. Consequently this structural effect should destabilize the CO/OO state and favour the  $T_{\text{IM}}$ -transition. Increase of the Mn–O bond length induces an opposite effect, favouring distortion of the  $\text{MnO}_6$  octahedra, i.e. the JT distortion, so the CO/OO state should be stabilized.

- (ii) The compression of the structure along the [010] direction (along the out-of-plane direction on STO), which appears simultaneously, results in a decrease of the  $^2$  Mn–O<sub>AX</sub>–Mn angle along this direction. Consequently, this decreases the bandwidth and stabilizes the CO/OO state.
- (iii) In the  $Pnma$  structure (such as that of NCMO), there are eight Mn–O<sub>EQ</sub>–Mn bonds against four Mn–O<sub>AX</sub>–Mn bonds. Thus, the bandwidth along Mn–O<sub>EQ</sub> is consistently larger than the bandwidth along the Mn–O<sub>AX</sub> direction, which indicates that the DE along the [101] direction prevails over that along the [010] direction [20].
- (iv) In view of these remarks, it is reasonable to assume that the substrate-induced strains modify in a first step the tilting of the octahedra, i.e. the Mn–O–Mn angles, and only in a second step the Mn–O bond lengths in the plane of the substrate.

For the larger film thicknesses ( $t > 2000 \text{ \AA}$ ), the cell parameters are close to those of the bulk, leading consequently to a tilting of the octahedra rather than a modification of the bond lengths. In other words, the variation of the Mn–O–Mn angles prevails over the variation of the Mn–O distances. Thus, as  $d_{101}$  increases the Mn–O<sub>EQ</sub>–Mn angles increase with respect to those in the bulk. In contrast, as  $d_{010}$  decreases the Mn–O<sub>AX</sub>–Mn angles decrease, resulting in an increase of the bandwidth along the [101] direction and a decrease of the bandwidth along the [010] direction. But, as pointed out above, the first effect prevails over the second one. As a consequence, the DE is favoured compared with that in the bulk, so the CO/OO state is less stable and  $T_{\text{IM}}$ -transition is obtained under a 7 T magnetic field, contrary to the case for the bulk.

As the thickness of the film decreases from  $2000 \text{ \AA}$ ,  $d_{101}$  increases significantly, so the Mn–O<sub>EQ</sub>–Mn bond angle reaches  $180^\circ$  rapidly and the Mn–O<sub>EQ</sub> bond length increases. The increase of the Mn–O<sub>EQ</sub> distance induces a JT distortion of the octahedra, stabilizing the

<sup>2</sup> See footnote 1.



CO/OO state to the detriment of the  $T_{\text{IM}}$ -transition. This explains why the  $T_{\text{CO}}$ -transition is more favoured as the thickness of the film decreases and the  $T_{\text{IM}}$ -transition under 7 T is less favoured, correspondingly. Finally, for smaller film thickness ( $t = 650 \text{ \AA}$ ),  $d_{101}$  is very close to the STO parameter, and the effect of the bond angle Mn–O<sub>EQ</sub> prevails over the Mn–O<sub>EQ</sub>–Mn effect, so the CO/OO state is the most stable. Note that the simultaneous decrease of  $d_{010}$ , i.e. decrease of Mn–O<sub>AX</sub>–Mn, also favours stabilization of the CO/OO state.

In the case of NCMO films grown on LAO, the substrate-induced strains lead in fact to rather similar effects. Indeed, one observes a compression along the [010] axis in the plane of the substrate. As shown in figure 5(b), this induces a decrease of the Mn–O<sub>AX</sub>–Mn angles and of the Mn–O<sub>AX</sub> bond lengths similar to what occurs for STO; an increase of the Mn–O<sub>EQ</sub>–Mn out-of-plane bond angle is induced, but in this case the increase of the Mn–O<sub>EQ</sub> bond distance does not prevail over the Mn–O<sub>EQ</sub>–Mn angle (not imposed by the substrate). For small thickness ( $t = 650 \text{ \AA}$ ), the  $T_{\text{IM}}$ -transition is favoured with respect to the CO/OO state.

#### 4. Conclusions

In conclusion, we grew high-quality thin films of Nd<sub>0.5</sub>Ca<sub>0.5</sub>MnO<sub>3</sub> on SrTiO<sub>3</sub> and LaAlO<sub>3</sub> using the PLD technique. We have shown that we are able to induce an insulator-to-metal transition at a magnetic field much lower than that required to produce the same effect in the corresponding bulk compound by modification of the structure through utilization of an appropriate substrate. Moreover the substrate-induced strains increase the Mn–O<sub>EQ</sub>–Mn bond angles on both LAO and STO substrates (even if the orientation of the film is different), favouring double exchange and consequently destabilizing the charge/orbital-ordered state leading to a decrease of the critical magnetic field as compared to that for the bulk.

#### References

- [1] Von Helmolt R, Wecker J, Holzapfel R, Schultz L and Samwer K 1993 *Phys. Rev. Lett.* **71** 2331  
McCormack M, Jin S, Tiefel T, Fleming R M, Philips J M and Ramesh R 1994 *Appl. Phys. Lett.* **64** 3045
- [2] Zener C 1951 *Phys. Rev.* **82** 403
- [3] Millis A J, Littlewood P B and Shraiman B 1995 *Phys. Rev. Lett.* **74** 5144
- [4] Wollan E O and Koehler W C 1955 *Phys. Rev.* **100** 545
- [5] Goodenough J B 1955 *Phys. Rev.* **100** 564
- [6] For a review see: Rao C N R, Arulraj A, Cheetham A K and Raveau B 2000 *J. Phys.: Condens. Matter* **12** R83
- [7] Vankatesan T, Rajeswari M, Dong Z-W, Ogale S B and Ramesh R 1998 *Phil. Trans. R. Soc.* **356** 1661  
Prellier W, Lecoœur Ph and Mercey B 2001 *J. Phys.: Condens. Matter* **13** R915
- [8] Chahara K, Ohno T, Kasai M and Kosono Y 1993 *Appl. Phys. Lett.* **63** 1990
- [9] Prellier W, Haghiri-Gosnet A M, Mercey B, Lecoœur Ph, Hervieu M, Simon Ch and Raveau B 2000 *Appl. Phys. Lett.* **77** 1023
- [10] Haghiri-Gosnet A M, Hervieu M, Simon Ch, Mercey B and Raveau B 2000 *J. Appl. Phys.* **88** 3545
- [11] Prellier W, Simon Ch, Haghiri-Gosnet A M, Mercey B and Raveau B 2000 *Phys. Rev. B* **62** R16 337
- [12] Zhang J, Tanaka H, Kanki T, Choi J and Kawai T 2001 *Phys. Rev. B* **64** 184404
- [13] Rauwel Buzin E, Prellier W, Simon Ch, Mercone S, Mercey B and Raveau B 2001 *Appl. Phys. Lett.* **79** 647
- [14] Tokunaga M, Miura N, Tomioka Y and Tokura Y 1998 *Phys. Rev. B* **57** 5259
- [15] Millange F, de Brion S and Chouteau G 2000 *Phys. Rev. B* **62** 5619
- [16] Murugavel P, Narayana C, Sood A K, Parashar S, Raju A R and Rao C N R 2000 *Europhys. Lett.* **52** 961
- [17] Respaud M, Llobet A, Frontera C, Ritter C, Broto J M, Rakoto H, Goiran M and Garcia-Muñoz J L 2000 *Phys. Rev. B* **61** 9014
- [18] Kuwahara H, Tomioka Y, Asamitsu A, Moritomo Y and Tokura Y 1995 *Science* **270** 961
- [19] Tomioka Y *et al* 1996 *Phys. Rev. B* **53** R1689
- [20] Woodward P M, Vogt T, Cox D E, Arulraj A, Rao C N R, Karena P and Cheetham A K 1998 *Chem. Mater.* **10** 3652  
Arulraj A, Santhosh P N, Gopalan R S, Guha A, Raychaudhuri A K, Kumar N and Rao C N R 1998 *J. Phys.: Condens. Matter* **10** 8497